

UNCLASSIFIED

Defense Technical Information Center  
Compilation Part Notice

ADP011803

TITLE: Semiconductor Quantum Dot Heterostructures [Growth and Applications]

DISTRIBUTION: Approved for public release, distribution unlimited

This paper is part of the following report:

TITLE: NATO Advanced Research Workshop on Nanostructured Films and Coatings. Series 3. High Technology - Volume 78

To order the complete compilation report, use: ADA399041

The component part is provided here to allow users access to individually authored sections of proceedings, annals, symposia, etc. However, the component should be considered within the context of the overall compilation report and not as a stand-alone technical report.

The following component part numbers comprise the compilation report:

ADP011800 thru ADP011832

UNCLASSIFIED

## SEMICONDUCTOR QUANTUM DOT HETEROSTRUCTURES (GROWTH AND APPLICATIONS)

V.M.USTINOV

*A.F.Ioffe Physico-Technical Institute*

*Politekhnikeskaya 26, 194021 St. Petersburg, Russia*

### Abstract

The reduction of dimensionality of the carrier motion in quantum nanostructures brings new, interesting effects in semiconductor physics. In addition, it opens an exciting possibility of improving the device performance. It has been predicted that the delta-function like density of states inherent for the objects with three-dimensional quantum confinement (quantum dots) should lead to the decrease in threshold current density, and improvement of its temperature stability (for semiconductor injection lasers when the quantum dot heterostructures are used as an active region).

In the present work we discuss the synthesis of InAs/GaAs quantum dots by using self-organization phenomena at the initial stages of strained layer heteroepitaxy. We show that the driving force for the island formation is strain accumulating during the deposition of the lattice mismatched material. Quantum dot size and shape are presented and their optical properties are discussed. The characteristics of quantum dot injection lasers are shown. The ways to reduce threshold current density and improve its temperature stability are demonstrated. The band-gap and strain engineering are shown to be effective tools for controlling the quantum dot optical emission range.

### 1. Introduction

When the motion of charge carriers is confined by the size of the order of de-Broigle wavelength of the particle the energy spectrum and other main characteristics of the system shows size dependence. This is a manifestation of the quantum size effect.

Semiconductor devices whose operation is based on the quantum size effect are currently widely used in various applications. For example, semiconductor diode lasers are used in optical fiber communications and compact disc players, high electron mobility transistors are used in satellite communication systems, etc. In these devices quantum size effect manifests itself in one direction, i.e. in the direction normal to the structure surface. Meanwhile, in the plane of the semiconductor layer the carrier motion is free. The new breakthrough in characteristics of semiconductor devices and appearance of new applications are associated with semiconductor structures where quantum size effect manifests itself in all three directions. These structures are called quantum dots (QDs).

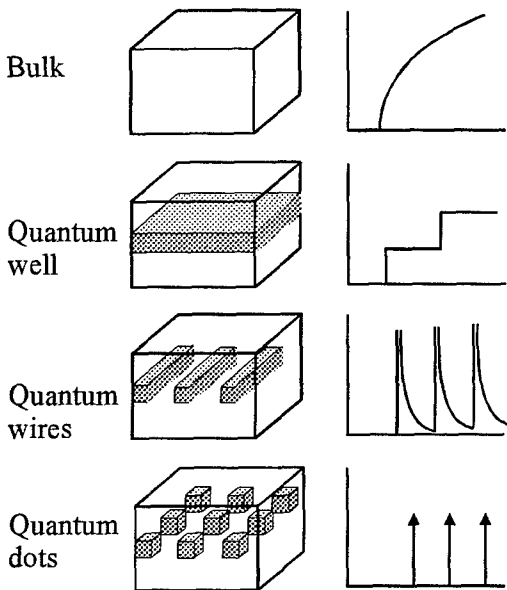


Figure 1. Effect of size quantization on density of states.

The structures of this kind are attractive mainly due to their energy spectrum which is essentially the set of discrete levels (Fig. 1). In this case thermal broadening is excluded and all carriers in the quantum dot array are characterized by the same energy if the quantum dot size is the same. It has been predicted [1,2] that this delta-function like density of states should lead to the drastic increase in gain and differential gain, decrease in threshold current density and the lack of its temperature dependence for semiconductor diode lasers.

To demonstrate their basic advantages, the main requirements to the structures synthesized are as follows [3]. The minimal size of a quantum dot is determined by the presence of at least one confined state. The maximal size

is limited by the lack of thermal population of adjacent states in a quantum dot. In addition, device applications exclude the exceptional amount of defects and dislocations as well as considerable interface recombination velocity. The quantum dot array should be uniformly dense to provide sufficient gain, since strong fluctuations in quantum dot size and shape would lead to the strong broadening of the spectrum. Extremely important is also the possibility for the matrix to provide the current flow and collection of carriers into the quantum dot states.

In the present work we discuss the synthesis of semiconductor quantum dots by using the effect of spontaneous transformation of the growth surface at the initial stages of lattice mismatched heteroepitaxy. The alternative methods of formation of quantum dots (e.g. etching the quantum well structures, growth in V-grooves or glass matrices) are beyond the scope of this work. Optical properties of self-organized quantum dots and their applications in diode lasers will also be discussed.

## 2. Synthesis of InAs/GaAs self-organized quantum dots

### 2.1. EPITAXIAL GROWTH MODES

Three possible mechanisms have been described so far in the theory of epitaxial growth: layer by layer or Frank van der Merwe (FvdM) growth mode, island or Volmer-Weber (VW), and island combined with layer or Stranski-Krastanov (SK) growth mode, Fig. 2. The type of epitaxial growth will be determined by the interface energy parameters and lattice mismatch. If the epitaxial layer and the substrate are lattice matched, the islands will be formed provided the surface energy of the substrate is less than the surface

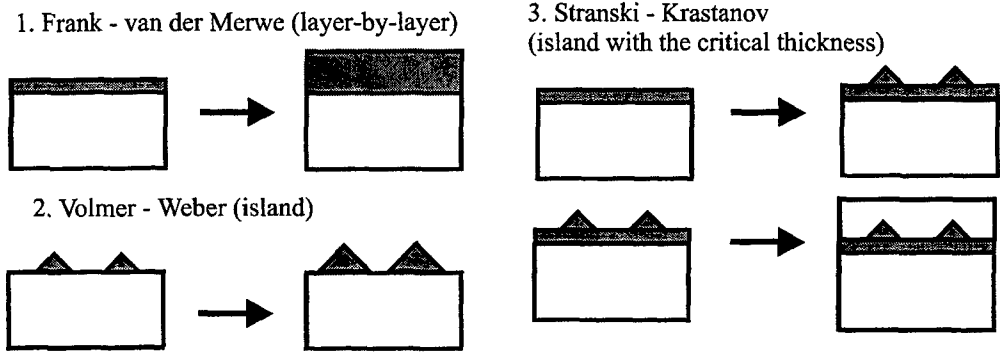


Figure 2. Possible mechanisms of epitaxial growth.

energy of the epitaxial layer and the interface energy. Variation of this energy relation leads to change in the growth from the VW to the FvdM mode. If the epitaxial layer and the substrate are lattice mismatched the growth initially proceeds in a layer by layer mode. However, increasing the layer thickness leads to the accumulation of large strain energy and it becomes energetically favorable for the system to reduce its energy by the formation of isolated islands due to strain relaxation. In the theory of the SK growth this process should be accompanied by the formation of misfit dislocations at the interface. However, it has been shown that for the lattice mismatched growth of semiconductors (e.g., Ge/Si, InAs/GaAs, etc) the critical layer thickness for the island growth is less than the critical thickness for the formation of dislocations [4, 5]. Thus, within a certain layer thickness coherent islands are formed on the growth surface. In this case the strain relaxation occurs either in the substrate adjacent to the island or in the island itself [4,5,6].

## 2.2. FORMATION OF ARRAYS OF InAs/GaAs SELF-ORGANIZED QUANTUM DOTS *IN SITU* BY MOLECULAR BEAM EPITAXIAL GROWTH

### 2.2.1. Structural characterization of quantum dots

The onset of the island growth mode upon the deposition of InAs on GaAs is usually monitored by high energy electron diffraction (HEED) patterns during the molecular beam epitaxial (MBE) growth (Fig. 3). The appearance of dashes and spots on the HEED pattern instead of streaks characteristic of the layer by layer growth is indicative of the formation of microscopic islands on the growth surface. If the deposition of InAs is interrupted at this stage, and the InAs islands obtained are overgrown by GaAs then the system of InAs islands in GaAs can be considered as a quantum dot array of low band-gap material in a large band-gap matrix.

Studying the initial stages of deposition of  $\text{In}_x\text{Ga}_{1-x}\text{As}$  on GaAs by HEED has shown that the increase in the In content ( $x$ ) in the epilayer leads to a decrease in the critical layer thickness for the island growth from 4 monolayers (ML) ( $x=0.5$ ) to 3 ML ( $x=0.6$ ) [7] and 1.7 ML ( $x=1$ ) [8].

Transmission electron microscopy (TEM) studies show that structural characteristics of  $\text{In}_x\text{Ga}_{1-x}\text{As}$  quantum dots in GaAs strongly depend on  $x$  and effective layer thickness, Fig. 4 [8]. Just exceeding the critical layer thickness the QD ensemble is characterized by pronounced lateral nonuniformities and small size of individual islands. Increasing the effective layer thickness to 4 ML (InAs) leads to the formation of about 60 Å high pyramidal quantum dots with square

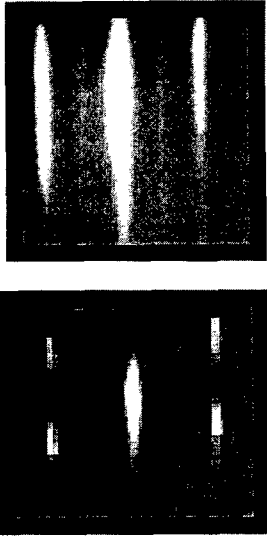


Figure 3. Change in HEED pattern with the deposition of InAs on GaAs surface due to the transition from layer-by-layer (1.6 ML, upper part) to island (1.7 ML, lower part) growth mode.

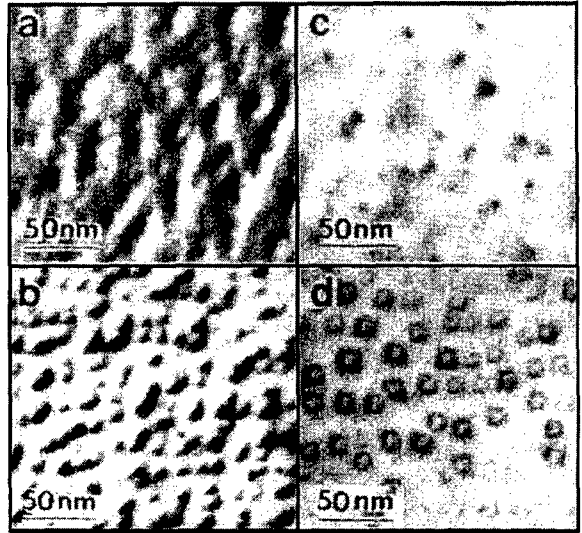


Figure 4. Plan-view TEM images of In(Ga)As QD arrays in a GaAs matrix: In<sub>0.5</sub>Ga<sub>0.5</sub>As QDs (3.3 ML (a), 7.3 ML (b)); InAs QDs (2 ML (c), 4 ML (d)).

bases ( $\sim 120$  Å). The islands form two-dimensional primitive square lattice, and their size distribution is relatively narrow (dispersion less than 20%).

Thus, the formation of InGaAs/GaAs self-organized quantum dots is controlled by the composition of the deposited layer and its effective thickness; the driving force for the formation of quantum dots is the strain energy accumulating upon the epitaxial growth of lattice mismatched semiconductor materials.

### 2.2.2. Optical properties of quantum dots

Coherent QDs usually show high (close to 100%) effectiveness of radiative recombination at low temperatures. The energy position of the photoluminescence (PL) peak strongly depends on the size of the islands [9]. Just after the formation of islands the PL peak becomes broadened and red shifted as compared to the quantum well case (Fig. 5a). Further increasing the effective thickness of InGaAs leads to gradual long wavelength shift of the PL line until the critical layer thickness for the dislocation formation is achieved (Fig. 5b). In this case the PL intensity is drastically decreased due to the large number of nonradiative recombination centers. The dots of smaller sizes usually exhibit a broader and weaker PL line as compared to the large dots with lower size dispersion. Integral PL intensity of the InAs/GaAs quantum dot heterostructures is almost independent of temperature until 100 K. However, increasing the temperature beyond 100 K leads to the decrease in the PL intensity characterized by the activation energy of about 80 – 90 meV. This value is close to the valence band discontinuity at the heterojunction InAs QD – GaAs matrix estimated theoretically [6] thereby indicating the effective evaporation of

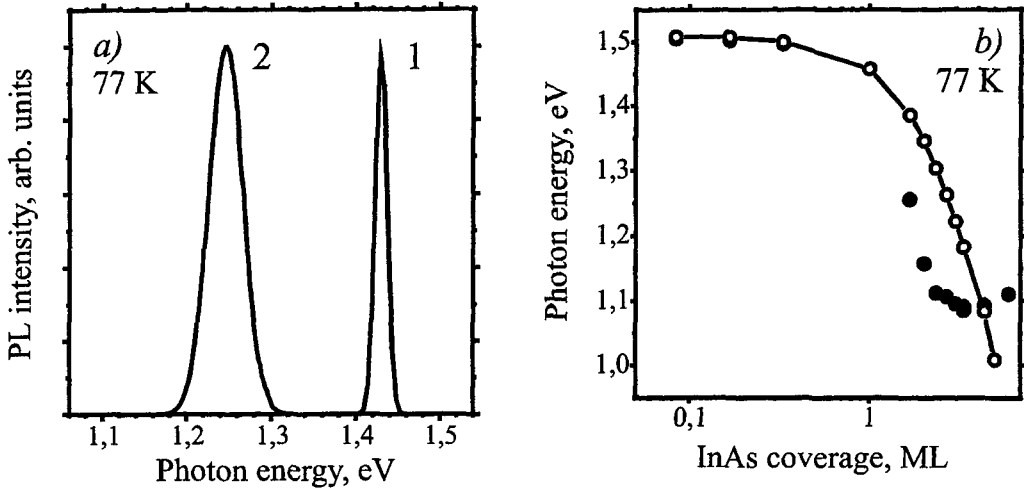


Figure 5. (a) PL spectra of heterostructures containing two-dimensional layer (curve 1) or QD array (curve 2) of InGaAs in a GaAs matrix. (b) Dependence of PL peak position from InAs insertion in GaAs: (●) measured experimentally; (○) calculated in assumption of two-dimensional coverage.

carriers from quantum dots at elevated temperatures [10]. Nevertheless, the room temperature PL intensity remains sufficiently high which allows the use of quantum dot structures in diode lasers.

### 2.2.3. Vertically coupled quantum dots

TEM studies have shown that typical InAs/GaAs quantum dots are characterized by relatively low aspect ratio (maximum base size  $\sim 140$  Å, maximum height  $\sim 60$  Å). Further increasing the effective thickness of deposited InAs leads to the formation of misfit dislocations. However, increasing the aspect ratio should lead to the increase in the carrier localization energy thereby suppressing the thermal evaporation of carriers from the QDs. This in turn should improve the room temperature characteristics of diode lasers.

It has been found that successive deposition of the InAs dot sheets and thin GaAs spacers leads to the formation of the islands of the subsequent sheet just above the islands of the previous sheet if the spacer thickness is less than or equal to the height of the island, Fig.6 [11]. The reason for this phenomenon is that the growth of the second InAs layer proceeds under the influence of the strain fields due to the presence of the previous QD sheet. This leads to the preferential migration of the In atoms to the places just above the location of the island of the previous layer.

The energy of the ground state transition has been found to depend on the number of the dot sheets and the spacer width. The PL peak shifts to the longer wavelengths with the increase in the number of QD sheets due to the decrease in the size quantization energy owing to the increase of the effective height of the quantum dot. The red shift of the PL line is also observed with the decrease in the spacer thickness due to the enhancement of the electronic coupling

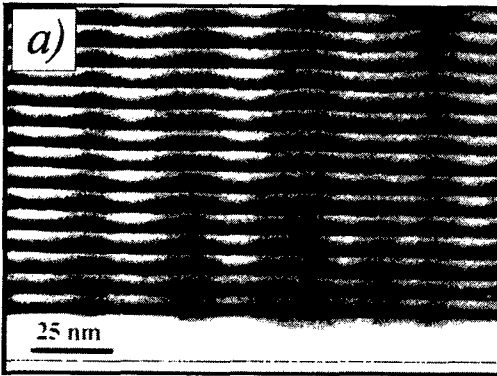
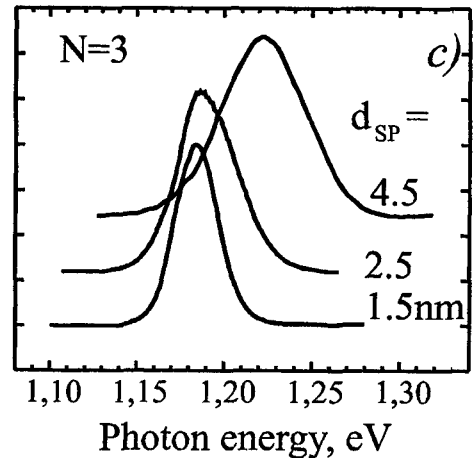
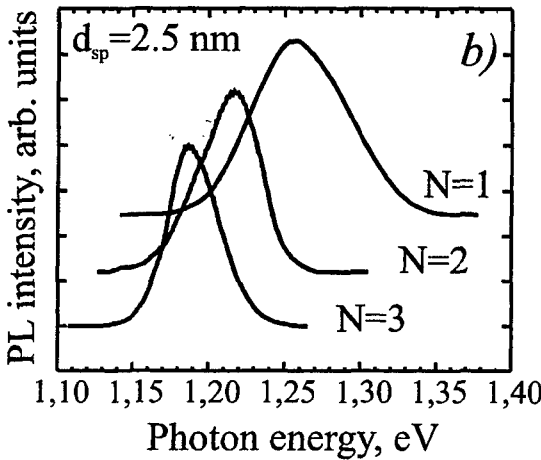


Figure 6. Cross-section TEM image of the structure containing more than 10 planes of InAs QDs separated by 5 nm-thick GaAs spacers (a) and evolution of PL spectrum of stacked QD array with the number of QD planes (b) and the spacer thickness (c).



between the dots of the adjacent layers. These effects are indicative of the fact that the vertically coupled quantum dot with strongly increased aspect ratio is a single quantum mechanical object characterized by a joint system of energy levels.

#### 2.2.4. Density of states spectrum of individual quantum dots

The PL spectrum of a quantum dot ensemble is a broad line (Fig. 5) which is the result of inhomogeneous broadening due to the size and shape fluctuations of the self-organized islands. Experimental evidence indicates that the energy spectrum of an individual quantum dot is a set of discrete energy levels due to three-dimensional quantization. This has been observed when studying cathodoluminescence (CL) under high spatial resolution of electron beam [12]. If only several tens of quantum dots are excited by a highly focused electron beam (under routine PL conditions  $10^7 - 10^8$  dots are within the laser spot) the CL spectrum is the set of ultra narrow lines (FWHM  $< 0.15$  meV) which is indicative of the lack of inhomogeneous broadening, Fig. 7. No increase in the width of the luminescence lines is observed with the increase in the temperature. This observation confirms that there is a lack of thermal broadening due to the delta function like density of states owing to the three dimensional quantization.

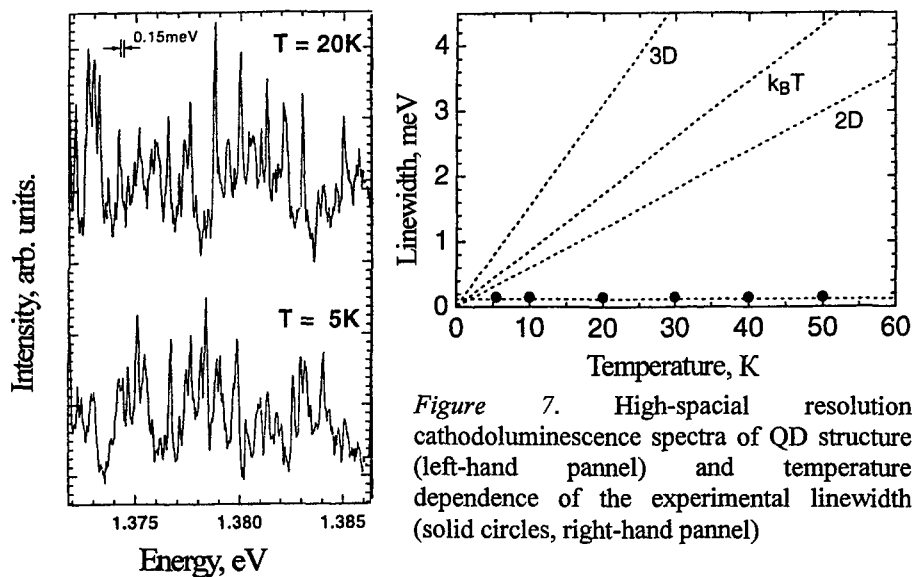


Figure 7. High-spatial resolution cathodoluminescence spectra of QD structure (left-hand panel) and temperature dependence of the experimental linewidth (solid circles, right-hand panel)

### 3. Formation of InAs quantum dots on silicon

Silicon is a key material in modern semiconductor technology. The important properties of silicon (high thermal conductivity, high stiffness, stable oxide formation, and developed technology for preparing inexpensive large-area dislocation-free substrates) make this material advantageous for numerous applications in microelectronics. On the contrary, the indirect bandgap of Si makes its application in optoelectronics very difficult. However, the luminescence efficiency of an indirect gap matrix can be dramatically improved by inserting a narrow- and direct-gap material (e.g. GaAs layers in AlAs). Nonequilibrium carriers are trapped in the direct-gap regions, and the luminescence efficiency may be extremely high, even

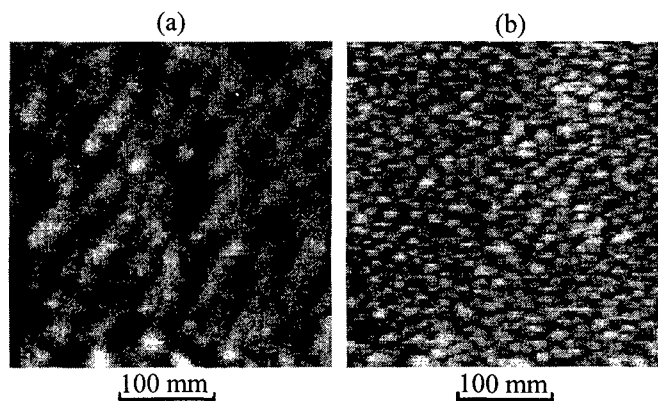


Figure 8. STM images of the surface morphology of InAs deposits on a Si (100) surface for 60 ML of InAs deposited at  $470^\circ\text{C}$  (a) and 5.5 ML InAs deposited at  $250^\circ\text{C}$  (b).



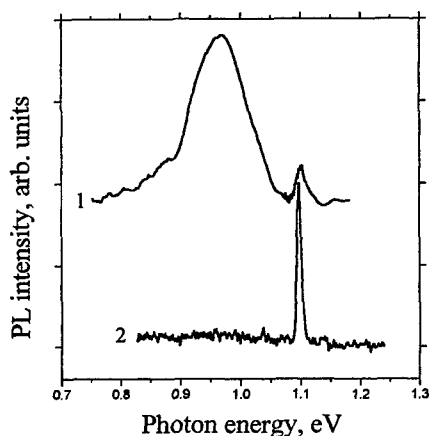


Figure 9. PL spectra of InAs QD array in a Si matrix (curve 1) and bare Si substrate (curve 2) at 77 K.

when the relative total thickness of the narrow gap material is small. Using the QD approach may be advantageous in overcoming the problems of lattice mismatch and anti-phase domains which are the main limiting factors for the growth of III-V materials on silicon.

When studying the growth regimes for InAs quantum dots on Si we have found that at moderate arsenic fluxes and substrate temperatures (470°C) (typical for the growth of InAs/GaAs quantum dots) InAs grows on Si (100) surface in the Stranski-Krastanow growth mode with the formation of mesoscopic dislocated clusters on top of a two-dimensional periodically corrugated InAs wetting layer. In contrast, at lower temperatures (250°C) a dense array of self-organized nanoscale InAs quantum dots of uniform size and shape is formed, Fig. 8. These quantum dots, when grown on a Si buffer layer and covered with a Si cap, give a PL line at about 1.3  $\mu\text{m}$ , Fig. 9 [13].

#### 4. Quantum dot diode lasers

##### 4.1. THRESHOLD CHARACTERISTICS

To study the diode lasers based on self-organized quantum dots, the quantum dot array was inserted into an active region of a GRIN SCH GaAs-(Al,Ga)As laser, Fig. 10. This allowed us to realize lasing via the ground state of quantum dots at low temperatures. Lasing wavelength was in the vicinity of the maximum of QD photoluminescence (PL) spectrum recorded at low excitation densities, and the threshold current density was found to be practically temperature insensitive in the temperature range up to  $\sim 100$  K. However, at higher temperatures we observed a steep increase in the threshold current density accompanied by a blue shift of lasing wavelength. Room temperature lasing energy was close to optical transition energy in a wetting layer (WL) [10]. Extremely high material and differential gain have been reported for these lasers, however, poor optical confinement factor led to moderate values of modal gain [14].

Important improvements in threshold characteristics of quantum dot diode lasers became possible due to the use of vertically coupled quantum dots in the active region [15]. These lasers show ground state lasing up to room temperature and the lasing wavelength follows the temperature dependence of the GaAs band-gap. The threshold current density steeply decreases and the range of its thermal stability increases with an increase in the number of QD layers (Fig. 11). The threshold current density ( $J_{th}$ ) is as low as 90-100 A/cm<sup>2</sup> at room temperature for  $N=10$  which is 10 times less than that for  $N=1$ .

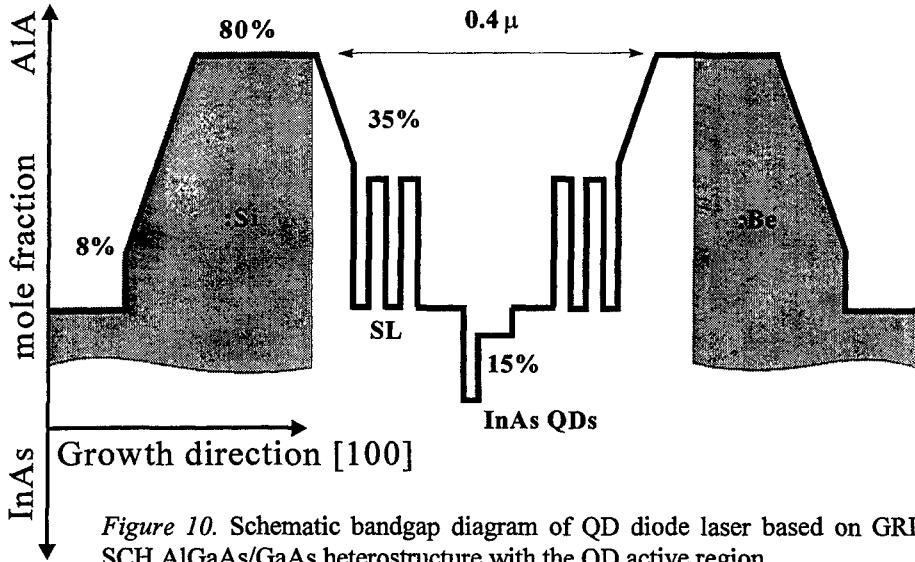


Figure 10. Schematic bandgap diagram of QD diode laser based on GRIN-SCH AlGaAs/GaAs heterostructure with the QD active region.

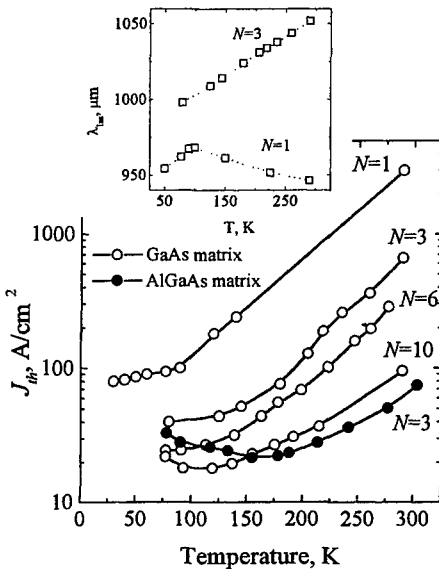


Figure 11. Temperature dependence of the threshold current density and the lasing wavelength (insert) for the lasers based on N layers of InAs QDs in GaAs or AlGaAs matrix.

Further decrease in threshold current density of quantum dot diode lasers was achieved by using the AlGaAs instead of the GaAs as a matrix for InGaAs QDs. This allowed for the increase in the barrier height for the carriers in the quantum dot states which reduces the carrier evaporation from quantum dots. The problem of low-temperature growth of AlGaAs is solved by *in situ* annealing during the high-temperature growth of the second emitter of the laser structure. This approach allowed us to achieve a room temperature threshold current density as low as 60 A/cm<sup>2</sup>, and a differential efficiency of more than 60% for a quantum dot diode laser [15]. The value of the threshold current density well corresponds to the best values reported for the quantum well lasers.

Studying the main mechanisms of internal carrier losses and leakage from the ground state of quantum dots has shown that the threshold current density can be reduced down to about 15 A/cm<sup>2</sup> at room temperature by reducing the non-radiative recombination and improving the carrier localization [16].

## 4.2. CONTINUOUS WAVE OPERATION OF QUANTUM DOT DIODE LASERS

The high quality of diode lasers, characterized by low threshold current density and reasonable differential efficiency, allowed us to demonstrate for the first time continuous wave (CW) operation of the QD lasers. Output power of about 1 W for the InGaAs/AlGaAs QD laser was reported [17].

One of the dominant mechanisms limiting output power of the semiconductor laser is spectral hole burning, associated with the finite capture time of charge carriers into the active states. Since the capture time into the ground state of In(Ga)As QDs is relatively large and the QDs themselves are characterized by a certain number of states determined by their surface density (typical value is  $3\div5\times10^{10}\text{ cm}^{-2}$ ), there is a maximum current capability of the QD active region. The increase in the surface density of QDs should allow us to increase the maximal possible current, which, in the turn, will increase the light output power. In [18] we have proposed the method to increase the surface density of QDs using denser InAlAs QDs as the

centers for stimulated formation of In(Ga)As QDs. The density of such composite vertically coupled QDs is set by the InAlAs islands ( $1\div1.5\times10^{11}\text{ cm}^{-2}$ ), whereas the optical transition energy is determined by the In(Ga)As QDs. Following this method we formed the active region of the laser which demonstrated maximum output power with uncoated facets in CW and pulsed regimes (10 °C) as high as 3.5 and 4.8 W, respectively, Fig. 12. The maximum value of output power was limited by catastrophic optical mirror damage (COMD). The internal loss for these diodes was estimated to be as low as  $1.3\pm0.3\text{ cm}^{-1}$ . The internal quantum efficiency was estimated to be about 75% [19]. Thus, QD lasers can be used for high-power applications.

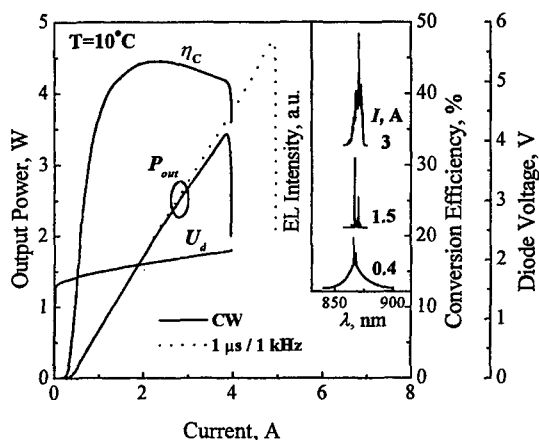


Figure 12. Output power,  $P_{out}$ , diode voltage,  $U_d$ , and conversion efficiency,  $\eta_c$ , vs drive current for the QD diode laser operating in CW regime at room temperature.

## 4.3. QUANTUM DOT DIODE LASERS FOR OPTICAL FIBER COMMUNICATIONS

Extension of the optical emission range available for the GaAs-based optoelectronic devices to  $1.3\text{ }\mu\text{m}$  is currently a subject of strong interest due to matching the transparency window of optical fibers. A number of attempts have been made to find an alternative to InGaAsP material system for laser diodes to overcome its strong temperature sensitivity due to insufficient electron confinement in the active region. Moreover, the use of GaAs-based lasers emitting at  $1.3\text{ }\mu\text{m}$  would eliminate the use of expensive InP substrates and the sophisticated technique of fusion of Bragg reflectors and active regions for vertical cavity devices. The approach based on

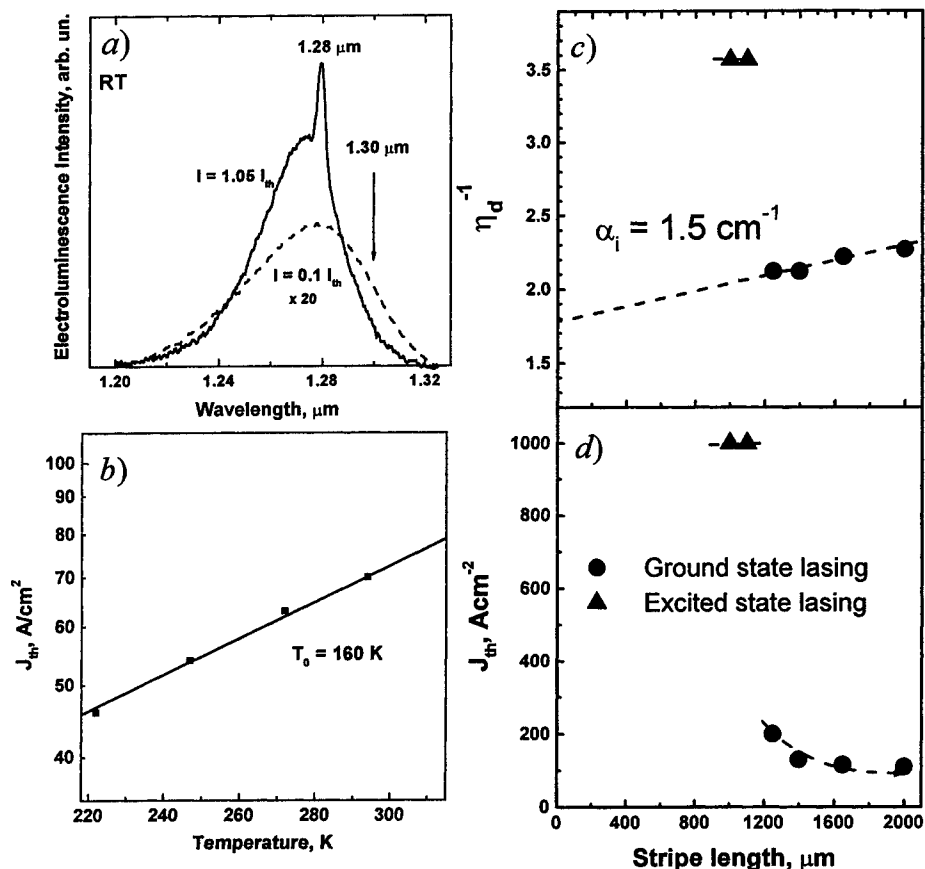


Figure 13. Electroluminescence (EL) spectra for four-side cleaved devices at room temperature (a), temperature dependence of the threshold current (b), dependence of the inverse differential efficiency (c) and the threshold current density (d) on the cavity length for the laser based on InAs QDs covered with InGaAs QW layer.

strained InGaAs/GaAs quantum well structures did not allow the necessary wavelength range to be reached due to the intrinsic limitation of the quantum well width associated with the border for pseudomorphic growth.

InAs/GaAs quantum dots are the promising candidates for extending the long wavelength border for the GaAs based light emitters. Once the InGaAs nanoscale islands are formed the pronounced red-shift of the luminescence peak position relative to that in strained InGaAs/GaAs quantum well is observed. We have proposed and realized a method to extend the optical emission range for the InGaAs/GaAs structures based on the effect of reduction of the energy of optical transition in a quantum dot when the bandgap of the surrounding matrix is decreased. We placed an InAs quantum dot (QD) array into external InGaAs strained quantum

well which allowed us to control the quantum dot emission wavelength by varying the InGaAs composition and to achieve the emission wavelength as long as 1.3  $\mu\text{m}$ , Fig. 13 [20]. Using these InAs/InGaAs/GaAs quantum dots in the active region of a diode laser allowed us to realize low threshold current density ( $J_{\text{th}} = 65 \text{ A/cm}^2$ ) operation near 1.3  $\mu\text{m}$  at room temperature. The lasing occurred via the QD ground state for cavity length  $L > 1 \text{ mm}$ . Differential efficiency is 40% and internal losses are  $1.5 \text{ cm}^{-1}$ . Characteristic temperature near RT is 160 K, Fig. 13, [21]. Thus, the GaAs-based QD laser emitting near 1.3  $\mu\text{m}$  demonstrated properties superior to those of InP-based QW devices.

#### 4.4. QUANTUM DOT DIODE LASERS FOR NEAR-IFRARED OPTICAL RANGE

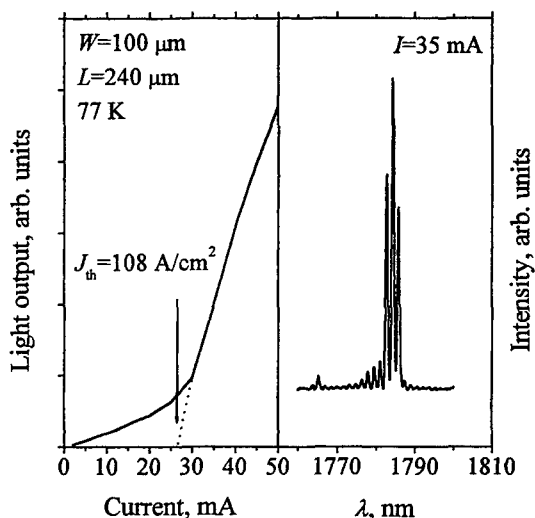


Figure 14. Light output vs drive current curve (left-hand panel) and above-threshold EL spectrum (right-hand panel) for 240- $\mu\text{m}$ -long stripe diode based on InAs QDs in an InGaAs/InP matrix.

Using the idea of the dependence of the quantum dot emission wavelength on the matrix band-gap allowed us to further increase the emission wavelength of a quantum dot laser. We used InGaAs ternary lattice matched to InP substrate as a matrix for InAs quantum dots. In this case the matrix band-gap was only  $\sim 0.8 \text{ eV}$  and consequently the QD emission wavelength should be considerably increased as compared to the InAs/GaAs case. We have shown experimentally that for the InAs/InGaAs/InP QDs the optical emission range can be extended to  $\sim 2 \mu\text{m}$  [22]. Having inserted these quantum dots into the InP/InAlAs/InGaAs laser structure we managed to observe lasing in the 77-200 K temperature range. Low threshold currents and emission wavelength at 1.8  $\mu\text{m}$  (77 K), Fig. 14, [23], show that the wavelength of the InAs QD lasers can be extended to the near-infrared optical range.

#### 5. Conclusions

InAs quantum dots have been successfully grown by MBE on GaAs, InP, and Si substrates. Growth regimes for the formation of coherent islands have been studied. Energy spectrum, structural, and optical properties have been evaluated. Diode lasers based on self-organized quantum dots have been fabricated and characterized. The possibility to obtain ultra low threshold current densities by optimizing the structural design and growth regimes has been demonstrated. Quantum dot lasers have demonstrated high output power performance comparable to the quantum well lasers. In addition, quantum dot lasers have extended the

optical emission range of the GaAs based lasers to wavelengths necessary for optical fiber communications.

## 6. Acknowledgements

This work in different parts is supported by Volkswagen Foundation (grant 1/73-631), INTAS (grants 96-0467 and 96-0242), BMBF 13 N 7231, NanOp CC, Russian Foundation for Basic Research (grant 99-02-16799), and the Program of Ministry of Science of Russia "Physics of Solid State Nanostructures.

The author is grateful to the Directors and Organizing Committee of the NATO Advanced Research Workshop "Nanostructured Films and Coatings" (Santorini, Greece, June 28-30, 1999) for financial support.

The author also gratefully acknowledges his colleagues whose contribution to this work was extremely important: A.Yu.Egorov, A.E.Zhukov, A.R.Kovsh, N.A.Maleev, S.S.Mikhrin, D.V.Denisov, M.V.Maximov, A.F.Tsatsul'nikov, I.L.Krestnikov, B.V.Volovik, D.A.Bedarev, Yu.M.Shernyakov, A.V.Lunev, E.Yu.Kondrat'eva, S.V.Zaitsev, N.Yu.Gordeev, V.I.Kopchatov, D.A.Lifshits, Yu.G.Musikhin, A.A.Suvorova, A.O.Kosogov, S.S.Ruvimov, N.A.Bert, P.S.Kop'ev, N.N.Ledentsov, and Zh.I.Alferov – Ioffe Institute, St. Petersburg, Russia; G.E.Cirlin and A.O.Golubok – Institute for Analytical Instrumentation, St. Petersburg, Russia; N.Kirstaedter, R.Heitz, M.Grundmann, and D.Bimberg – Technical University of Berlin, Berlin, Germany; P. Werner – Max-Planck Institute, Halle, Germany; Z.Liliental-Weber and E.R.Weber – Lawrence Berkeley National Laboratory, Berkeley, CA, USA.

## 7. References

1. Arakawa, Y. and Sakaki, H. (1982) Multidimensional quantum well laser and temperature dependence of its threshold current, *Appl. Phys. Lett.* **40**, 939-941.
2. Asada, M., Miyamoto, Y., and Suematsu, Y. (1986) Gain and the threshold of the three-dimensional quantum-box lasers, *J. Quantum Electron.* **QE-22**, 1915-1921.
3. Ledentsov, N.N. (1996) Ordered arrays of quantum dots, in M. Scheffler and R. Zimmerman (eds.), *Proceedings of the 23<sup>rd</sup> International Conference on the Physics of Semiconductors* **1**, Berlin, Germany, 19-26.
4. Eaglesham, D.J. and Cerullo, M. (1990) Dislocation-free Stranski-Krastanow growth of Ge on Si (100), *Phys. Rev. Lett.* **64**, 1943-1946.
5. Guha, S., Madhukar, A., and Rajkumar, K.C. (1990) Onset of incoherency and defect introduction in the initial stages of molecular beam epitaxial growth of highly strained  $\text{In}_x\text{Ga}_{1-x}\text{As}$  on GaAs (100), *Appl. Phys. Lett.* **57**, 2110-2112.
6. Grundmann, M., Stier, O., and Bimberg, D., (1995) InAs/GaAs pyramidal quantum dots: Strain distribution, optical phonons, and electronic structure, *Phys. Rev. B* **52**, 11969-11981.
7. Egorov, A.Yu., Zhukov, A.E., Kop'ev, P.S., et al. (1994) Effect of deposition conditions on the formation of (In,Ga)As quantum clusters in a GaAs matrix, *Semiconductors* **28**, 809-811.

- 8 Ruvimov, S.S., Werner, P., Scheerschmidt, K., et al. (1995) Structural characterization of (In,Ga)As quantum dots in a GaAs matrix, *Phys. Rev. B* **51**, 14766-14769.
- 9 Egorov, A.Yu., Zhukov, A.E., Kop'ev, P.S., et al. (1996) Optical emission range of structures with strained InAs quantum dots in GaAs, *Semiconductors* **30**, 707-710.
- 10 Bimberg, D., Ledentsov, N.N., Grundmann, M., et al. (1996) InAs-GaAs quantum pyramid lasers: in situ growth, radiative lifetimes, and polarization properties, *Jpn. J. Appl. Phys., Part 1* **35**, 1311-1319.
- 11 Ustinov, V.M., Egorov, A.Yu., Zhukov, A.E., et al. (1996) Formation of stacked self-assembled InAs quantum dots in GaAs matrix for laser applications, *Mat. Res. Soc. Symp. Proc.* **417**, 141-146.
- 12 Grundmann, M., Christen, J., Ledentsov, N.N., et al. (1995) Ultranarrow luminescence lines from single quantum dots, *Phys. Rev. Lett.* **74**, 4043-4046.
- 13 Cirlin, G.E., Dubrovskii, V.G., Petrov, V.N., et al. (1998) Formation of InAs quantum dots on a silicon (100) surface, *Semicond. Sci. Technol.* **13** 1262-1265.
- 14 Kirstaedter, N., Schmidt, O.G., Ledentsov, N.N., et al. (1996) Gain and differential gain of single layer InAs/GaAs quantum dot injection lasers, *Appl. Phys. Lett.* **69**, 1226-1228.
- 15 Ustinov, V.M., Egorov, A.Yu., Kovsh, A.R., et al. (1997) Low-threshold injection lasers based on vertically coupled quantum dots, *J. Cryst. Growth* **175**, 689-695.
- 16 Zaitsev, S.V., Gordeev, N.Yu., Kopchatov V.I., et al. (1997) Vertically coupled quantum dot lasers: first device oriented structures with high internal quantum efficiency, *Jpn. J. Appl. Phys. Part 1* **36**, 4219-4220.
- 17 Maximov, M.V., Shernyakov, Yu.M., Tsatsul'nikov, A.F., et al. (1998) High-power continuous-wave operation of a InGaAs/AlGaAs quantum dot laser, *J. Appl. Phys.* **83**, 5561-5563.
- 18 Kovsh, A.R., Zhukov, A.E., Egorov, A.Yu., et al. (1998) MBE growth of composite (In,Al)As/(In,Ga)As vertically coupled quantum dots and their application in injection lasers, *Proc. of 10<sup>th</sup> Int. Conf. MBE, Abstract Book*, 175. (to be published in *J. Cryst. Growth*, 1999).
- 19 Kovsh, A.R., Zhukov, A.E., Livshits, D.A., et al. (1999) 3.5 W CW operation of a quantum dot laser, *Electron. Lett.* (to be published)
- 20 Ustinov, V.M., Maleev, N.A., Zhukov, A.E., et al. (1999) InAs/InGaAs quantum dot structures on GaAs substrates emitting at 1.3  $\mu\text{m}$ , *Appl. Phys. Lett.* **74**, 2815-2817.
- 21 Shernyakov, Yu. M., Bedarev, D.A., Kondrat'eva, E.Yu., et al. (1999) 1.3  $\mu\text{m}$  GaAs-based laser using quantum dots obtained by activated spinodal decomposition, *Electron. Lett.*, in press
- 22 Ustinov, V.M., Zhukov, A.E., Tsatsul'nikov, A.F., et al. (1997) Arrays of strained InAs quantum dots in an (In,Ga)As matrix grown on InP substrates by molecular beam epitaxy, *Semiconductors* **31**, 1080-1083.
- 23 Ustinov, V.M., Zhukov, A.E., Egorov, A.Yu., et al. (1998) Low threshold quantum dot injection laser emitting at 1.9  $\mu\text{m}$ , *Electron. Lett.* **34**, 670-672.